Electronic Supplementary Material (ESI) for Physical Chemistry Chemical Physics.
This journal is © the Owner Societies 2023

Wave function analyses of scandium-doped aluminium clusters, Al_nSc (n = 1–24), and their CO_2 fixation abilities. Electronic Supplementary Information

José Manuel Guevara-Vela[a], Arturo Sauza-de la Vega[b], Miguel Gallegos[c], Ángel Martín Pendás[c], Tomás Rocha-Rinza[d,*]

[a]*Departamento de Química Física Aplicada. Universidad Autónoma de Madrid, Madrid 28049, Spain.*
[b]*Department of Chemistry, University of Chicago, Chicago, IL 60637, USA*
[c]*Department of Analytical and Physical Chemistry, University of Oviedo, E-33006, Oviedo, Spain.*
[d]*Instituto de Química, Universidad Nacional Autónoma de México, Circuito Exterior, Ciudad Universitaria, Delegación Coyoacán C.P. 04510, Ciudad de México, Mexico.*

[*]To whom correspondence should be addressed: trocha@iquimica.com.mx

1. Theoretical background

In this section, we briefly survey the QTAIM and IQA methods of wave function analyses exploited in this work. Succinctly, the QTAIM[1] utilises the topology of the electron density of a system, to perform a partition of the 3D real space of a molecule or molecular cluster under investigation into atoms or basins denoted as Ω_{A}, $\Omega_{\mathrm{B}}\ldots$ Since the electron density is the expectation value of a Dirac observable, i.e., $\varrho(\boldsymbol{r}) = \left\langle \sum_{i=1}^{N} \delta(\boldsymbol{r}_i - \boldsymbol{r}) \right\rangle$, wherein N is the number of electrons in the system, the QTAIM results are independent on how the approximation of the electronic wave function is constructed, e.g., using orthogonal Slater determinants or non-orthogonal valence-bond functions. Furthermore, the QTAIM basins are quantum subsystems for which one can compute the expectation value of quantum-mechanical observables such as, the electron population ($N_{\Omega_{\mathrm{A}}}$) and energy ($E^{\Omega_{\mathrm{A}}}_{\mathrm{QTAIM}}$) among others. These average values can be used to determine other relevant atomic properties. For instance, given the atomic electron population, it is straightforward to calculate the QTAIM atomic charge as,

$$q(\Omega_{\mathrm{A}}) = Z_{\Omega_{\mathrm{A}}} - N_{\Omega_{\mathrm{A}}}, \tag{S1}$$

wherein $Z_{\Omega_{\mathrm{A}}}$ and $N_{\Omega_{\mathrm{A}}}$ are respectively the nuclear charge and the electron population of Ω_{A}. One can also determine the covariance between electron populations of two atomic basins, say Ω_{A} and Ω_{B}. Such covariance is used as the basis for a measure of covalency in the interaction between Ω_{A} and Ω_{B}, known as delocalisation index,[2]

$$\delta^{\Omega_{\mathrm{A}}\Omega_{\mathrm{B}}} = -2\mathrm{cov}(N_{\Omega_{\mathrm{A}}}, N_{\Omega_{\mathrm{B}}}). \tag{S2}$$

We say in this case that there are $\delta^{\Omega_{\mathrm{A}}\Omega_{\mathrm{B}}}$ electrons delocalised between Ω_{A} and Ω_{B}.

Herein, we also considered the IQA energy partition of the electronic energy in net and interaction energies:[3,4]

$$E = \sum_{\Omega_{\mathrm{A}}} E^{\Omega_{\mathrm{A}}}_{\mathrm{net}} + \frac{1}{2} \sum_{\Omega_{\mathrm{A}} \neq \Omega_{\mathrm{B}}} E^{\Omega_{\mathrm{A}}\Omega_{\mathrm{B}}}_{\mathrm{int}}. \tag{S3}$$

The IQA energy decomposition has been successfully exploited to study the chemical bonding under many different circumstances[5–8]. The IQA interaction energies, $E_{\rm int}^{\Omega_{\rm A}\Omega_{\rm B}}$ can be further divided into classical and exchange-correlation contributions,

$$E_{\rm int}^{\Omega_{\rm A}\Omega_{\rm B}} = V_{\rm cl}^{\Omega_{\rm A}\Omega_{\rm B}} + V_{\rm xc}^{\Omega_{\rm A}\Omega_{\rm B}}, \tag{S4}$$

in which $V_{\rm cl}^{\Omega_{\rm A}\Omega_{\rm B}}$ and $V_{\rm xc}^{\Omega_{\rm A}\Omega_{\rm B}}$ represent the ionic and covalent components to the interaction between $\Omega_{\rm A}$ and $\Omega_{\rm B}$ respectively. Finally, we also considered the decomposition of the formation energy of a given cluster $\mathscr{G}\cdots\mathscr{H}\cdots\mathscr{I}\cdots$

$$\mathscr{G} + \mathscr{H} + \mathscr{I} + \cdots \rightleftharpoons \mathscr{G}\cdots\mathscr{H}\cdots\mathscr{I}\cdots, \quad \Delta E, \tag{S5}$$

as a sum of the deformation and interaction energies of the species comprising $\mathscr{G}\cdots\mathscr{H}\cdots\mathscr{I}\cdots$,[3,4,9]

$$\Delta E = \sum_{\mathscr{G}} E_{\rm def}^{\mathscr{G}} + \frac{1}{2}\sum_{\mathscr{G}\neq\mathscr{H}} E_{\rm int}^{\mathscr{G}\mathscr{H}}. \tag{S6}$$

$E_{\rm def}^{\mathscr{G}}$ accounts for the difference of energy between $\mathscr{G}$ within the cluster $\mathscr{G}\cdots\mathscr{H}\cdots\mathscr{I}\cdots$ and the equilibrium energy of isolated $\mathscr{G}$,

$$E_{\rm def}^{\mathscr{G}} = E_{\rm net}^{\mathscr{G}} - E_{\rm iso}^{\mathscr{G}}, \tag{S7}$$

while $E_{\rm int}^{\mathscr{G}\mathscr{H}}$ is the pairwise sum of interaction energies of the atoms comprising $\mathscr{G}$ and $\mathscr{H}$,

$$E_{\rm int}^{\mathscr{G}\mathscr{H}} = \sum_{{\rm A}\in\mathscr{G}}\sum_{{\rm B}\in\mathscr{H}} E_{\rm int}^{\rm AB}. \tag{S8}$$

Furthermore, $E_{\rm int}^{\mathscr{G}\mathscr{H}}$ can also be decomposed in classical and exchange-correlation components,

$$E_{\rm int}^{\mathscr{G}\mathscr{H}} = V_{\rm cl}^{\mathscr{G}\mathscr{H}} + V_{\rm xc}^{\mathscr{G}\mathscr{H}}, \tag{S9}$$

as put forward in formula (S4).

Finally, we considered the deviation of planarity[10]

$$Q_c = \sqrt{\frac{\sum_i^N \left(\boldsymbol{m}\cdot(\boldsymbol{r}_i - \overline{\boldsymbol{r}})^2\right)}{N}} \tag{S10}$$

for the investigated Al_n and Al_nSc clusters. Concerning the quantities in the RHS of equation (S10), N is the number of atoms in the system, $\overline{\boldsymbol{r}}$ is the position of their center of mass and $\boldsymbol{r}_i$ is the position of atom i n the system. Finally, $\boldsymbol{m}$ is the eigenvector with the smallest eigenvalue of the moments matrix,

$$\mathbf{q} = \begin{pmatrix} \sum_i^N (x_i - \overline{x})^2 & \sum_i^N (x_i - \overline{x})(y_i - \overline{y}) & \sum_i^N (x_i - \overline{x})(z_i - \overline{z}) \\ \sum_i^N (y_i - \overline{y})(x_i - \overline{x}) & \sum_i^N (y_i - \overline{y})^2 & \sum_i^N (y_i - \overline{y})(z_i - \overline{z}) \\ \sum_i^N (z_i - \overline{z})(x_i - \overline{x}) & \sum_i^N (z_i - \overline{z})(y_i - \overline{y}) & \sum_i^N (z_i - \overline{z})^2 \end{pmatrix}. \tag{S11}$$

A value $Q_c = 0$ indicates that all the atoms are located in a plane, while high values of Q_c indicate large departures from planarity.

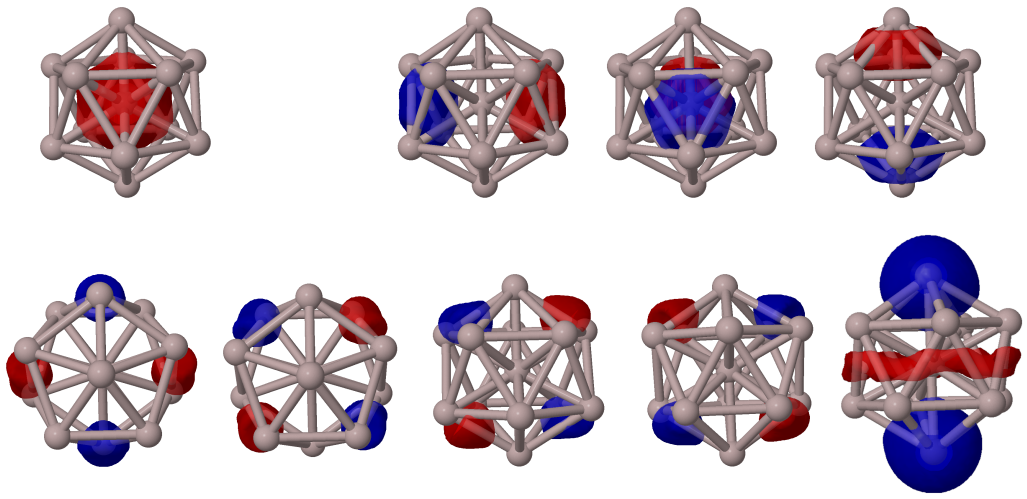

Figure S1: Adaptive orbitals based on real space natural density partitioning[21,22] of Al_{13}.

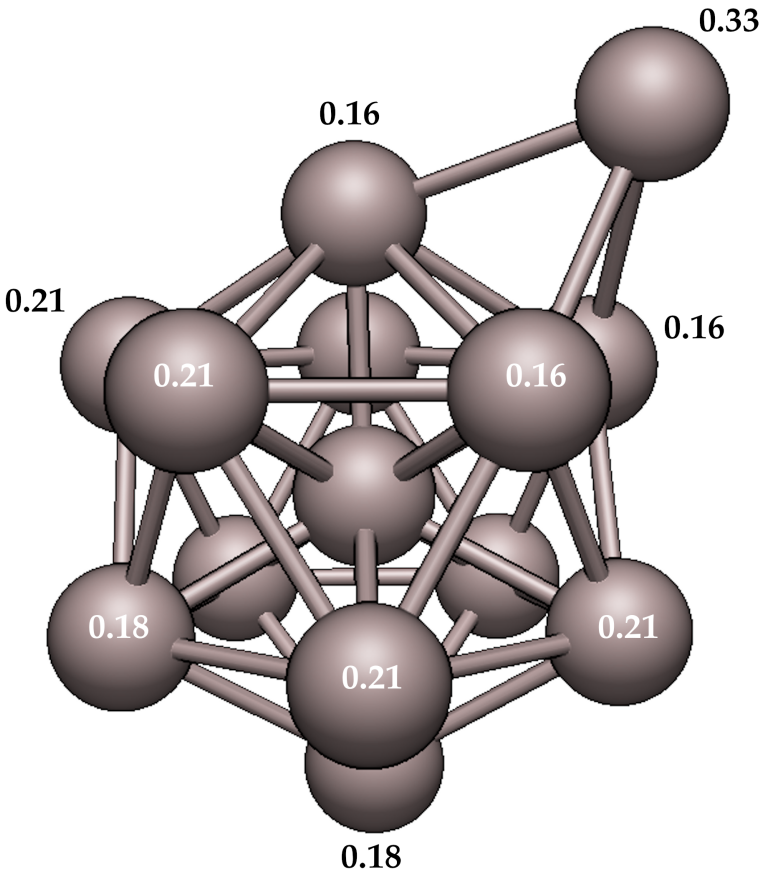

Figure S2: QTAIM charges within the icosahedral structure of Al_{14} for (i) the Al atoms interacting with and (ii) those Al basins furthest way from the exterior aluminium.

2. xyz files

In this link

https://doi.org/10.5281/zenodo.7834708

the interested reader can download the xyz files of the local minima of the Al_n and $Al_{n-1}Sc$ (n = 2–25) cluster addressed in this investigation.

References

[1] R. F. W. Bader, *Atoms in molecules: A Quantum Theory*, Oxford University Press, **1990**.

[2] B. Silvi, *Phys. Chem. Chem. Phys.* **2004**, *6*, 256–260.

[3] M. A. Blanco, A. Martín Pendás, E. Francisco, *J. Chem. Theory Comput.* **2005**, *1*, 1096–1109.

[4] E. Francisco, A. Martín Pendás, M. A. Blanco, *J. Chem. Theory Comput.* **2005**, *2*, 90–102.

[5] I. Alkorta, I. Mata, E. Molins, E. Espinosa, *Chem. Eur. J.* **2016**, *22*, 9226–9234.

[6] C. Foroutan-Nejad, *Angew. Chem. Int. Ed.* **2020**, *59*, 20900–20903.

[7] L. J. Duarte, W. E. Richter, R. E. Bruns, P. L. A. Popelier, *J. Phys. Chem. A* **2021**, *125*, 8615–8625.

[8] S. S. Karachi, K. Eskandari, *J. Comput. Chem.* **2022**, *44*, 962–968.

[9] A. Martín Pendás, M. A. Blanco, E. Francisco, *J. Chem. Phys.* **2006**, *125*, 184112.

[10] N. C. Firth, N. Brown, J. Blagg, *J. Chem. Inf. Model* **2012**, *52*, 2516–2525.

[11] J. P. Perdew, K. Burke, M. Ernzerhof, *Phys. Rev. Lett.* **1996**, *77*, 3865–3868.

[12] F. Weigend, R. Ahlrichs, *Phys. Chem. Chem. Phys.* **2005**, *7*, 3297–3305.

[13] R. P. F. Kanters, K. J. Donald, *J. Chem. Theory Comput.* **2014**, *10*, 5729–5737.

[14] M. Ernzerhof, J. P. Perdew, *J. Chem. Phys.* **1998**, *109*, 3313.

[15] C. Adamo, V. Barone, *J. Chem. Phys.* **1999**, *110*, 6158–6170.

[16] F. Neese, *Wiley Interdiscip. Rev. Comput. Mol. Sci.* **2017**, *8*, e1327.

[17] G. M. J. Barca, C. Bertoni, L. Carrington, D. Datta, N. De Silva, J. E. Deustua, D. G. Fedorov, J. R. Gour, A. O. Gunina, E. Guidez, T. Harville, S. Irle, J. Ivanic, K. Kowalski, S. S. Leang, H. Li, W. Li, J. J. Lutz, I. Magoulas, J. Mato, V. Mironov, H. Nakata, B. Q. Pham, P. Piecuch, D. Poole, S. R. Pruitt, A. P. Rendell, L. B. Roskop, K. Ruedenberg, T. Sattasathuchana, M. W. Schmidt, J. Shen, L. Slipchenko, M. Sosonkina, V. Sundriyal, A. Tiwari, J. L. Galvez Vallejo, B. Westheimer, M. Wloch, P. Xu, F. Zahariev, M. S. Gordon, *The Journal of Chemical Physics* **2020**, *152*, 154102.

[18] T. A. Keith, *AIMAll (Version 19.02.13)*, TK Gristmill Software, Overland Park KS, USA, 2019 (aim.tkgristmill.com).

[19] M. D. Hanwell, D. E. Curtis, D. C. Lonie, T. Vandermeersch, E. Zurek, G. R. Hutchison, *J. Cheminform.* **2012**, *4*, 2946–4.

[20] W. Humphrey, A. Dalke, K. Schulten, *Journal of Molecular Graphics* **1996**, *14*, 33–38.

[21] E. Francisco, A. Costales, M. Menéndez-Herrero, Á. Martín Pendás, *J. Phys. Chem. A* **2021**, *125*, 4013–4025.

[22] D. Y. Zubarev, A. I. Boldyrev, *Phys. Chem. Chem. Phys.* **2008**, *10*, 5207.